

## IV.A.11 Reversible Hydrogen Storage Materials – Structure, Chemistry, and Electronic Structure

Ian M. Robertson (Primary Contact),  
Duane D. Johnson, Angus Rockett,  
Dennis D. Graham, Stephen D. House,  
and Pamela Martin  
University of Illinois, Urbana-Champaign (UIUC)  
Department of Materials Science and Engineering  
1304 West Green Street  
Urbana, IL 61801  
Phone: (217) 333-6776; Fax: (217) 333-2736  
E-mail: ianr@illinois.edu

DOE Technology Development Manager:  
Ned Stetson  
Phone: (202) 586-9995; Fax: (202) 586-9811  
E-mail: Ned.Stetson@ee.doe.gov

DOE Project Officer: Paul Bakke  
Phone: (303) 275-4916; Fax: (303) 275-4753  
E-mail: Paul.Bakke@go.doe.gov

Contract Number: DE FC36-05GO15064

Project Start Date: March 1, 2005  
Project End Date: February 26, 2010

### Technical Targets

This project is conducting fundamental experimental and theoretical studies of candidate lightweight systems for on-board regeneration. Insights gained from these studies will be applied toward the design and synthesis of hydrogen storage materials that meet the following DOE 2010 hydrogen storage targets:

- Cost: \$4/kWh net
- Specific energy: 1.5 kWh/kg
- Energy density: 0.9 kWh/L



### Introduction

Our work at UIUC focuses on resolving issues within current hydrogen storage materials using a combination of electronic structure calculations and state-of-the-art compositional and structural characterization methods. We tie together theoretical understanding of electronic, enthalpic, thermodynamic, and surface effects affecting performance of storage materials with microcompositional and microstructural experimental analysis, coordinated with other efforts from MHCoe partners. These efforts enable a more efficient approach to designing a new system with the required properties.

Established partnerships in previous fiscal years with the following groups (Sandia National Laboratories [SNL], HRL, University of Pittsburgh (Pitt), Georgia Tech, and University of Hawaii). We expanded our collaborations to include Brookhaven National Laboratory. These partnerships have provided and will continue to produce meaningful results for the investigation of structure and chemistry for hydrogen storage materials.

### Objectives

The main focus of UIUC within the Metal Hydride Center of Excellence (MHCoe) is:

- Advance the understanding of the microstructural and modeling characteristics of complex hydrides.
- Provide feedback and knowledge to partners within MHCoe framework.
- Provide more reliable theoretical methods to assess hydrogen-storage materials, including key issues affecting materials under study.

### Technical Barriers

This project addresses the following technical barriers from the Storage section of the Hydrogen, Fuel Cells and Infrastructure Technologies Program Multi-Year Research, Development and Demonstration Plan:

- (E) Charging/Discharging Rates
- (P) Lack of Understanding of Hydrogen Physisorption and Chemisorption

### Approach

We employ state-of-the-art characterization tools to investigate the microstructural and microchemical changes that occur in candidate material systems during the uptake and release of hydrogen. The characterization is coupled with first-principles, electronic-structure and thermodynamic theoretical techniques to predict and assess meta-stable and stable phases, as well as surface effects that can poison or limit kinetics. Electronic-structure and thermodynamic calculations are used to enhance the understanding of MHCoe experimental characterization results on

candidate systems. The theoretical work at UIUC is coordinated closely with MHCoe theory partners, as well as experimental efforts. This combined theoretical/characterization effort provides fundamental insight to the processes governing hydrogen uptake and release.

## Results

### Theory Efforts

We are continuing studies with several Center members. A selection of this work includes:

- Density functional theory studies of stability of intermediate phase in  $\text{Ca}(\text{BH}_4)_2$  and  $\text{Mg}(\text{BH}_4)_2$  systems (with SNL) are continuing. We have found a stable intermediate  $\text{CaB}_{12}\text{H}_{12}$  closo-molecule, relative to segregation back to constituents used to obtain initial  $\text{Ca}(\text{BH}_4)_2$  (with SNL). The reaction energies, summarized in Table 1, show that there are several (certainly more than have been found previously) near-degenerate structures, which is the origin of the irreversibility issues. A series of images showing different monoclinic unit cells of the material is shown in Figure 1. For the most stable structure (e), the space group is P2/m (No. 10). The lattice parameters of the base-centered monoclinic unit cell are  $a=11.71 \text{ \AA}$ ,  $b=7.02 \text{ \AA}$ ,  $c=11.16 \text{ \AA}$  and  $\beta=89.96^\circ$  (angle between  $a$  and  $c$  unit cell vectors). We have submitted for publication a paper that includes both the experimental and theoretical results that discusses why this system is irreversible.

**TABLE 1.** Reaction energies (product minus reactant) of dehydrogenation of  $\text{Ca}(\text{BH}_4)_2$ . Zero-point energies (bolded) are included in the top most values. Reaction 4 (with closo  $\text{CaB}_{12}\text{H}_{12}$ ) is lowest in energy, while reaction 3 is lower per mol- $\text{H}_2$ . There are multiple related reactions of type 4 due to the importance of ionic charge, i.e. (a) NaCl-based monoclinic (C2/m); (b) distorted ZnS-type zinc-blende structure (P2); (c) disordered hcp Wurtzite structure (Pm); and (d) distorted hcp Wurtzite structure (C2/m); and (e) distorted hcp Wurtzite structure (P2/m).

	Reaction	$\Delta\text{H}(0 \text{ K})$	
		(eV)	(kJ/mol- $\text{H}_2$ )
1	$\text{Ca}(\text{BH}_4)_2 \rightarrow \text{Ca}+2\text{B}+4\text{H}_2$	3.45	83.3
2	$\text{Ca}(\text{BH}_4)_2 \rightarrow \text{CaH}_2+2\text{B}+3\text{H}_2$	1.80	57.8
3	$\text{Ca}(\text{BH}_4)_2 \rightarrow \frac{2}{3}\text{CaH}_2+\frac{1}{3}\text{CaB}_6+\frac{10}{3}\text{H}_2$	1.34	38.9
4	$\text{Ca}(\text{BH}_4)_2 \rightarrow \frac{5}{6}\text{CaH}_2+\frac{1}{6}\text{CaB}_{12}\text{H}_{12}+\frac{13}{6}\text{H}_2$	--	--
4a	" (C2/m 50)	0.97	43.3
4b	" (P2 50)	0.92	41.2
4c	" (Pm 100)	0.90	39.9
4d	" (C2/m 100)	0.89	39.7
4e	" (P2/m 100)	0.88	39.4

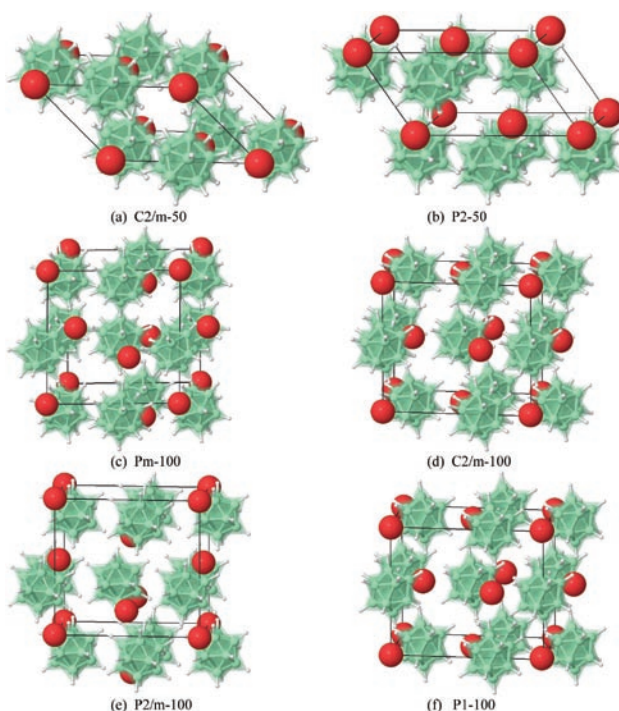


**FIGURE 1.** Unit cells of  $\text{CaB}_{12}\text{H}_{12}$  polymorphs. Labels refer to symmetry groups: (a) NaCl-based (C2/m); (b) distorted (zinc-blende) ZnS (P2); and four distorted Wurtzite with point-group symmetries of (c) Pm; (d) C2/m; (e) P2/m; and (f) P1.

- X-ray diffraction studies of desolvated and dehydrogenated  $\text{Ca}(\text{BH}_4)_2$  samples obtained from SNL were performed to identify the phases present. Shown in Figure 2, the peaks for the desolvated  $\text{Ca}(\text{BH}_4)_2$  phase matches well with those from the standard for  $\alpha\text{-Ca}(\text{BH}_4)_2$  structure. After dehydrogenation, the  $\text{Ca}(\text{BH}_4)_2$  peaks mostly disappear and new peaks, which match well with the standard  $\text{CaH}_2$  pattern, appear. These X-ray diffraction results indicate that, save for  $\text{CaH}_2$ , there are no identifiable crystalline intermediate phases present in the dehydrogenated samples. Electron diffraction from a single particle shows weak crystalline diffraction spots superimposed on a diffuse background. This pattern is consistent with the particle being amorphous with a low volume fraction of small crystalline regions. The diffraction pattern could not be identified which precluded identification of the crystalline material. Chemical analysis via electron energy loss spectroscopy, as noted in the previous report, confirms that there is no significant redistribution of the elements within the particle. Hence, the dehydrogenated intermediate phase is amorphous predominantly with no significant compositional modifications.
- In the  $\text{CaB}_{12}\text{H}_{12}$  polymorphs, Figure 1, B is narrowly distributed inside the closo-molecule, yielding

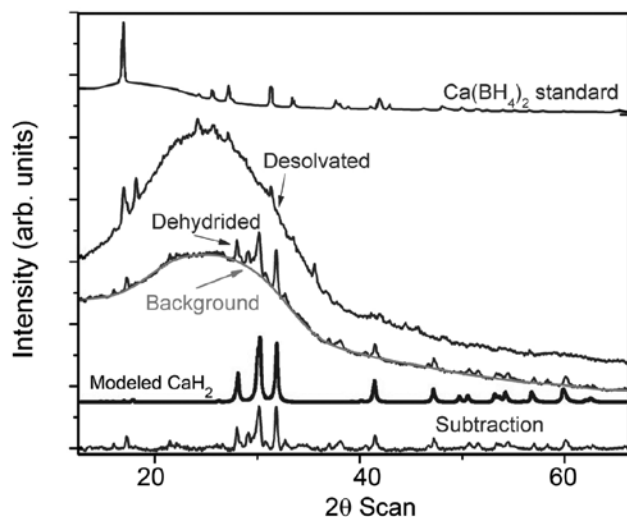


**FIGURE 2.** X-ray diffraction patterns from desolvated and dehydrogenated  $\text{Ca}(\text{BH}_4)_2$ , with comparison to a standard (Fddd symmetry) from Miwa *et al* [1]. After background subtraction, modeled  $\text{CaH}_2$  pattern matches closely with our dehydrogenated data. The few weak, unmatched peaks (e.g.,  $2\theta \sim 29^\circ$ ) do not fit to any Ca- or B-based compound, such as  $\text{CaB}_6$ .

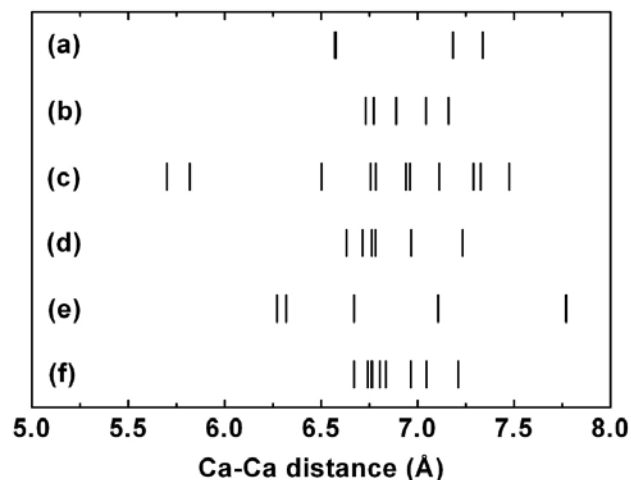


**FIGURE 3.** Nearest-neighbor Ca-Ca bond distributions for  $\text{CaB}_{12}\text{H}_{12}$  in Figure 1, where (f) is similar to (d), but with rotated closomolecule units, showing the sensitivity of Ca-Ca bond distribution to closomolecule orientation.

a similar bond distribution for all polymorphs, with the only difference being in orientation. The largest difference is the positions of the Ca ions. The Ca-Ca bond-length distributions for these structures, Figure 3, varies from  $5.5\text{Å}$  to  $7.6\text{Å}$ . Since the structures are close in energy, multiple polymorphs are present, the competition of which leads to a broad distribution of Ca-Ca bond-lengths. Arrangement of the polymorphs such that there is no long-range order, coupled with the broad Ca-Ca

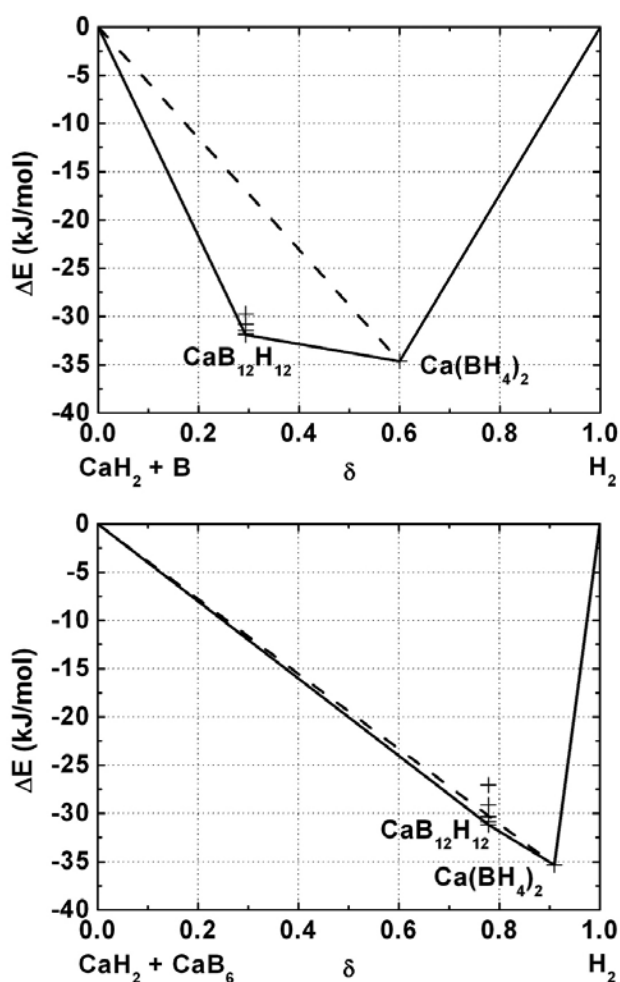


**FIGURE 4.** Formation enthalpy ( $\text{kJ/mol}$ ) of  $\text{CaB}_x\text{H}_y$  versus  $\delta$  (at%  $\text{H}_2$ ) relative to (a)  $\text{CaH}_2 + \text{B}$  and (b)  $\text{CaH}_2 + \text{CaB}_6$ . For  $\text{CaB}_{12}\text{H}_{12}$  and  $\text{Ca}(\text{BH}_4)_2$   $\delta$  in (a) is  $5/17$  and  $3/5$ , and (b)  $7/9$  and  $10/11$ , respectively. Dashed line indicates how much more stable  $\text{CaB}_{12}\text{H}_{12}$  is relative to the constituent materials at each end of the line. Energies for  $\text{CaB}_{12}\text{H}_{12}$  involve multiple structures (Figure 1) marked by “+” signs.

bond length provides a rationale explanation for the electron and X-ray diffraction data.

- Recent calculations, Figure 4, show that  $\text{CaB}_{12}\text{H}_{12}$  is slightly lower in energy than a mixture of  $\text{Ca}(\text{BH}_4)_2$  and  $\text{CaB}_6 + \text{CaH}_2$ . The energy barrier along the segregation pathway ( $\text{CaB}_6 + \text{CaH}_2$ ) and the  $\text{CaB}_{12}\text{H}_{12}$  intermediate state is much larger than that between  $\text{CaB}_{12}\text{H}_{12}$  and  $\text{Ca}(\text{BH}_4)_2$ , indicating that the  $\text{CaB}_{12}\text{H}_{12}$  intermediate phases are energetically favorable. The large chemical potential required to get back to “ $\text{CaH}_2 + \text{B} + \text{H}_2$ ” from  $\text{CaB}_{12}\text{H}_{12}$ , and similarly from  $\text{Ca}(\text{BH}_4)_2$ , inhibits reversibility, making the reverse reaction unlikely except at temperatures and pressure too high for practical use in hydrogen storage applications. Thus,  $\text{Ca}(\text{BH}_4)_2$  has limited viability as a reversible storage material

for on-board storage for vehicles, but may still be promising as a chemical hydride.

### Experimental Efforts

On the experimental side we continue to work with several of our partners. A selection of the work done includes:

- In conjunction with Brookhaven National Laboratory, we have investigated the location of the catalytic Ti in  $\text{AlH}_3$ -triethylenediamine (TEDA). This material is the first hydrogen reversible alane produced and the results shown here are the first characterization results on this system. Through a combination of transmission electron microscopy and scanning electron microscopy (SEM), we have shown that large fibers exist and these show a strong aluminum and nitrogen peak, which is consistent with the formation of  $\text{AlH}_3$ -TEDA. A representative image of these fibers is shown in Figure 5. In association with the fibers are occasional “bunches” of nodular particles which are composed primarily of Al, also indicated in Figure 5. These crystals are formed in solution with TEDA under hydrogen pressure.
- Within the nodular Al crystals, there is a high concentration of Ti that was not observed in the fibers. The  $\text{AlH}_3$ -TEDA fibers have no detectable Ti, but the nodular crystals show Ti being present at a concentration of 0.4 at%. This stands in stark

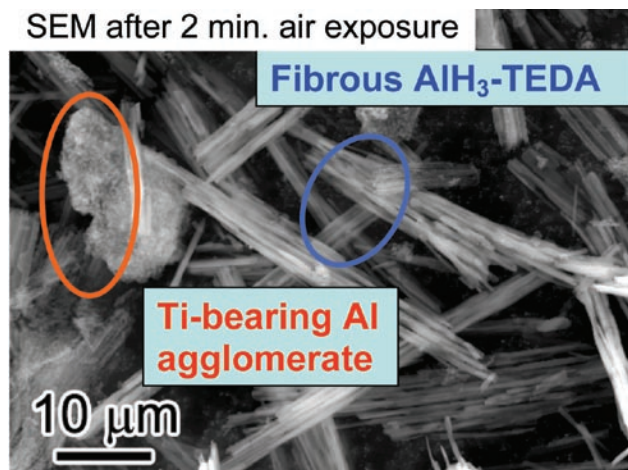


**FIGURE 5.** Scanning electron microscope image of  $\text{AlH}_3$ -TEDA (triethyldiamine) which has been doped with 0.1 mol %  $\text{TiCl}_3$ . Within the large fibrous crystals, both Al and nitrogen are strongly identified, confirming that this material is the  $\text{AlH}_3$  adduct described in Graetz *et al* [2]. This phase of material is formed in the liquid state under hydrogen pressure in a glovebox. Previously unknown small Al clusters or grains were also found in association with this material. These clusters were identified as essentially pure Al with 0.4 at % Ti. These clusters have high amounts of Ti with respect to how much was added to the material. This suggests that the TEDA is very selective for  $\text{AlH}_3$ .

contrast to the doping concentration, which was 0.1 at% Ti. This result suggests that the Ti, when the material is placed under hydrogen pressure, assists the formation and departure of  $\text{AlH}_3$  from the surface of the material. As soon as an  $\text{AlH}_3$  molecule is formed at the surface, it is scavenged from the material and Ti is left behind. This result has implications for understanding the catalytic activity in  $\text{NaAlH}_4$  and suggests that the action of Na is irrelevant and that the only important aspect is the interaction of Ti with the Al surface. In addition, the amount of Ti present in the remaining nodules is higher than that added, which means it has concentrated in the nodules. In conjunction with past research on the role of doping in  $\text{NaAlH}_4$ , this suggests that much of the added Ti becomes inert or is lost. This result suggests that the amount of necessary titanium participating in the catalytic process is low and is <0.1 at%. Efforts are ongoing to identify partners who can provide low-temperature distillation to separate  $\text{AlH}_3$ -ethylene diamine from the Al crystals for mass spectrometry to evaluate the Ti concentration necessary for catalysis.

- In collaboration with SNL, we are investigating the use of metal organic frameworks (MOF) as a medium to contain hydrogen storage materials. Theoretical proposals have suggested that making particles very small (<5 nm) may enhance the kinetics of hydrogen uptake and release from these storage materials. MOFs are porous, building-block structures with pore sizes on the order of a few nanometers. By infiltrating hydrogen storage material into MOFs, their particle size should be constrained by the pore sizes of the frameworks. There is a great need, however, to know where the hydrogen storage material is located within the MOF. That is, is the storage material on the surface or located within the MOF?
- Electron tomography reconstructions of both cured and uncured Ag-MOF systems were produced, Figure 6 and 7; this system was studied simply to demonstrate proof of concept. In both systems, the Ag particles were dispersed throughout the framework and not restricted to the surface. Nanowire structures were reported to be present in the uncured system, but their exact structure was unknown. From the reconstruction, Figure 8, it is obvious that the “nanowire” structure is neither extensive nor uniform, but has a morphology resembling a row of “sintered” Ag particles. The techniques used to visualize this material, of which a primitive form was previously demonstrated with Ni particles in  $\text{MgH}_2$ , were advanced further during these experiments and now will be applied to hydrogen storage MOFs provided by SNL.

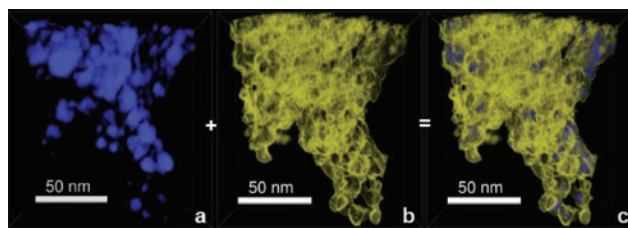


**FIGURE 6.** Tomographic reconstruction of a cured Ag-MOF specimen with contrast set to show (a) only the Ag particles, (b) only the framework, and (c) Ag and framework combined. The Ag particles are clearly spread throughout the inside of the MOF, not segregated to the surface.

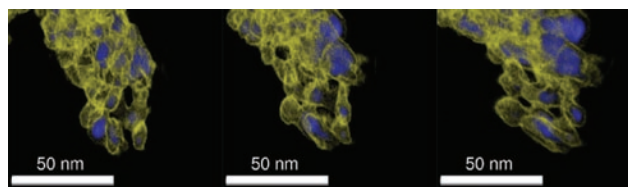


**FIGURE 7.** Series of higher magnification images of the reconstruction of the cured Ag-MOF system from Figure 6 as it is being tilted. Relationship between the Ag particles and MOF is easily understood.

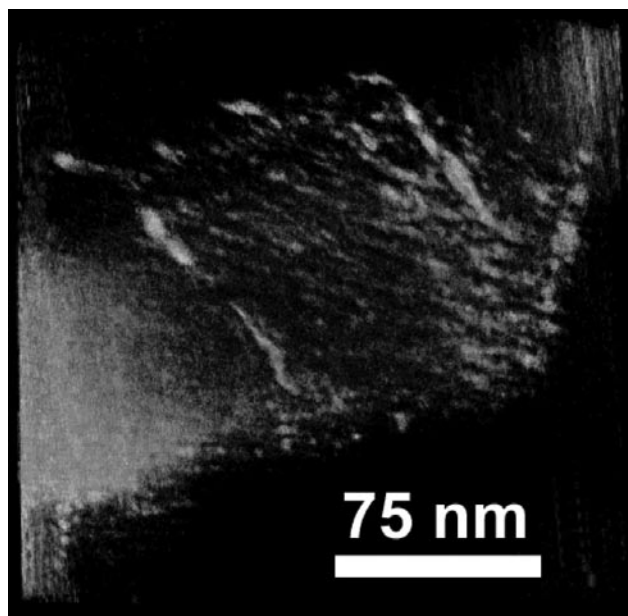


**FIGURE 8.** Tomographic reconstruction of an uncured Ag-MOF specimen with contrast set to show purported "nanowire" structures. The loss of depth information in 2-dimensional imaging led to confusion about actual structure of these wires, which is dispelled by the 3-dimensional reconstruction.

- Installation and calibration of new equipment for the variable temperature scanning tunneling microscope at the University of Illinois has been completed. After surmounting difficulties involving

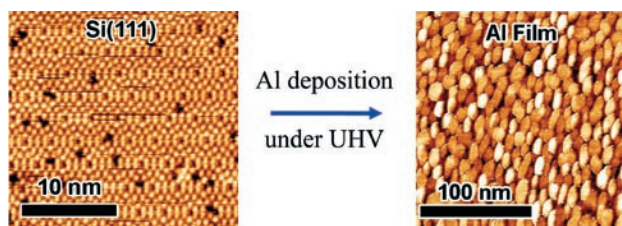


**FIGURE 9.** Epitaxial thin films of Al (right) are grown on Si(111) substrates (left) under ultra-high vacuum conditions. Si(111) with epitaxial later chosen due to known growth conditions and similarity to other hydrogen-storage materials. (See, e.g., Hasan, *et al.* [3]).

substrate preparation and installation of the deposition apparatus, test runs were promising, leading to final preparation of epitaxial thin films of Al on Si(111) substrates, Figure 9, of which initial resistivity measurements for suitability were made last quarter. These Al films will be used to investigate the properties of undoped and Ti-doped Al surfaces in the presence of hydrogen in a controlled fashion, without mechanical alloying, to answer the fundamental question about the atomic-level mechanisms of hydrogen uptake and release from clean and poisoned surfaces. Future work may expand these initial efforts to other systems.

## Conclusions and Future Directions

- Identified high-T phase of  $\text{LiBH}_4$  via molecular dynamics modeling and matched with experiment data.
- Completed work on theory to address reliably the thermodynamics in molecular solids, using molecular dynamics modeling of  $\text{LiBH}_4$  as case study (see publications).
- Completed joint theory effort on poisoning effects on Li-, Na-, and K-based borohydrides that showed that disassociation of  $\text{H}_2\text{O}$  to hydroxides ( $-\text{OH}$ ) limited reversibility in  $\text{LiBH}_4$  (see publications, with SNL, HRL, Pitt, Georgia Tech).
- Proposed possible Mg/Li alanate storage system reactions to avoid poisoning issues (with SNL, HRL, Pitt/Georgia Tech).
- Addressed, both experimentally and theoretically, the stability of observed intermediate phase in  $\text{Ca}(\text{BH}_4)_2$  and  $\text{Mg}(\text{BH}_4)_2$  systems (with SNL). Found stable  $\text{Ca}(\text{B}_{12}\text{H}_{12})_2$  intermediate relative to those used to obtain initial  $\text{Ca}(\text{BH}_4)_2$  (with SNL). A manuscript has been submitted for publication.
- Completed grain-size analysis of complex hydrides.
- We initiated study of  $\text{MgH}_2$  and Mg nanoparticles and their interaction with carbon-based supports, such as aerogels. We find similar results to de Jonge *et al.* [4] for free clusters, showing extremely distorted particles even with 31 molecular units, in

distinction to studies by Larsson et al. [5] which did not permit global relaxations. We provided these to Mark Allendorf and collaborators in Berkeley to help seed one of their quantum Monte Carlo investigations for cluster/support investigations.

- The concentration of Ti needed to activate the  $\text{AlH}_3$ -TEDA system is significantly less than that added, with losses of Ti of up 90% being found.

Future directions include:

- Continue surface science study for reaction of  $\text{H}_2$  with clean and poisoned Al surfaces.
- Complete study of  $\text{Ca}(\text{BH}_4)_2$  systems (with SNL), both experiment and theory.
- Continue work on evaluation of ball milling for mixing of catalysts.
- Continue investigation of hydrogen storage MOFs using tomography.
- Continue our investigation of the compositional difference in the  $\text{Al}_3$ -TEDA system.

For Fiscal Year 2010 we will continue experimental studies of the microchemical and microstructural changes occurring in different candidate systems that are supplied by the various partners. In addition to electron diffraction and energy dispersive spectroscopy analysis, electron energy loss spectroscopy will continue to be a powerful tool to be applied to partner systems to identify electronic states within the materials. In addition, the recent addition of electron tomography to our suite of tools allows 3-dimensional information to be obtained from ball-milled materials. This allows the position, surface or embedded, of the catalyst particles to be determined. In addition, a new effort to analyze surface states that is ramping up this year will continue to provide useful results in FY 2010.

Electronic-structure methods will be used to support the surface-science experiments planned on Al (cleaned and poisoned). In addition, we will complete several studies involving stability of bulk  $\text{Ca}(\text{BH}_4)_2$  and clusters of Mg and  $\text{MgH}_2$ . We will complete studies of nanocluster structures of  $\text{MgH}_2$  and  $\text{NaAlH}_4$  with and without interactions to a carbon support (approximating interactions with aerogels). We are determining the effects of nanosize and support interactions on H desorption. Results of these studies may require experimental verification and we will collaborate with partners as appropriate. Additional calculations will be performed with input from partners regarding key issues.

We will continue to develop and enhance our electron tomography techniques as we apply it to

hydrogen storage MOF systems. Current limitations on data set size and reconstruction speeds have been overcome with the purchase of a new computer workstation designed for such processor- and memory-intensive applications.

## FY 2009 Publications/Presentations

1. N.A. Zarkevich, and D.D. Johnson, "Predicting Enthalpies of Molecular Substances: exemplified via  $\text{LiBH}_4$ ". *Physical Review Letters* 100, 040602-4 (2008).
2. N.A. Zarkevich, Teck L. Tan, L-L. Wang and D.D. Johnson, "Low-energy antiphase boundaries, degenerate superstructures, and phase stability in frustrated Ising model and Ag-Au alloys," *Phys. Rev. B* 77, 144208-9 (2008).
3. Bing Dai, Rees B. Rankin and J. Karl Johnson, Mark D. Allendorf, David S. Sholl, N.A. Zarkevich, and D.D. Johnson, "Influence of Surface Reactions on Complex Hydride Reversibility," *J. Phys. Chem. C*, 112 (46), 18270-18279 (2008).
4. L.-L. Wang, D.D. Graham, E. Ronnebro, I.M. Robertson, D.D. Johnson. "On the reversibility of  $\text{Ca}(\text{BH}_4)_2$  hydrogen-storage reactions: microstructural and chemical characterization via experiment and theory," submitted.
5. R.J.T. Houk, B.W. Jacobs, F.E.G. Marquez, A.A. Talin, M.D. Allendorf, S. House, D.D. Graham I.M. Robertson, N. Ferralis, R. Maboudian. "Solution-Based Infiltration and Templated Growth of Very Small Ag-clusters in Metal Organic Frameworks for SERS Generation: Evidence That Larger-than-Pore Particles are Imaging Artifacts," submitted to *Nanoletters*.
6. N.A. Zarkevich, S.V. Alapati, D. Sholl, and D.D. Johnson, "Prediction of enthalpies and van't Hoff plots of multiphase chemical reactions", in preparation.
7. D.D. Graham, J. Graetz, J. Reilly, I.M. Robertson. "Electron microscopy of  $\text{AlH}_3$ : location of dopant in reversible Alane." In preparation.
8. D.D. Graham, I.M. Robertson. "Evaluation of ball milling for incorporation of in catalysts in Mg and Ca complex hydride-storage materials". In preparation.

## References

1. Miwa, K. *et al*, *Physical Review B* **2006**, 74, 155122.
2. Graetz *et al*. Direct and reversible synthesis of  $\text{AlH}_3$ -triethylenediamine from Al and  $\text{H}_2$ . *Journal of Phys. Chem. C*, **111** (2007) 19152.
3. Hansen et al. *Vacuum* 41 (1990) 1121.
4. de Jonge et al. *J. Am. Chem. Soc.* 127, 16675 (2005).
5. Larsson et al, *PNAS* (2007).